Graphene Oxide Liquid Crystal Membranes in Protic Ionic Liquid for Nanofiltration

ACS APPLIED NANO MATERIALS

Subscriber access provided by King Abdullah University of Science and Technology Library

Article

Graphene Oxide Liquid Crystal Membranes in Protic Ionic Liquid for Nanofiltration

Dinesh Mahalingam, Shaofei Wang, and Suzana P. Nunes

ACS Appl. Nano Mater., **Just Accepted Manuscript** • DOI: 10.1021/acsanm.8b00927 • Publication Date (Web): 04 Sep 2018

ACS Publications

is published by the American Chemical Society. 1155 Sixteenth Street N.W., Washington, DC 20036

Graphene Oxide Liquid Crystal Membranes in Protic Ionic Liquid for Nanofiltration

*Dinesh K Mahalingam, Shaofei Wang and Suzana P Nunes**

King Abdullah University of Science and Technology (KAUST), Biological and Environmental Science and Engineering Division (BESE), Water Desalination and Reuse Center,

23955-6900 Thuwal, Saudi Arabia

*Corresponding author: Suzana P Nunes, E-mail: suzana.nunes@kaust.edu.sa

KEYWORDS: graphene oxide, liquid crystals, protic ionic liquids, membranes, nanofiltration

ABSTRACT: Graphene oxide (GO) liquid crystals are of great interest for membrane preparation. Vacuum filtration has been frequently adopted as small-scale manufacturing method. The main challenge is to obtain thin and robust layers with high permeation and selectivity by methods that could be applied in large scale. GO liquid crystals are mostly formed by dispersion in water. For the first time, we demonstrate that GO can form lyotropic liquid crystalline nematic phase dispersions in protic ionic liquid and be fabricated as membranes for nanofiltration. The well-balanced electrostatic interaction between ionic liquid and GO promotes and stabilizes the alignment of GO nanosheets even when concentrations as low as 9 mg GO /mL are used, providing the ideal rheology for the dispersion casting and membrane preparation. Robust membranes with GO layers as thick as 1 μm with high permeance (37 L m^{-2} h^{-1} bar^{-1}) and 99.9 % rejection of dyes with molecular weight 697 g/mol were obtained. We confirmed the liquid crystal formation by the detection of birefringence and the rheological behavior and explained the liquid crystal formation as an interplay between hydrogen bonding and electrostatic interactions.

The growing demand of drinking water and the need of water reuse in the agriculture and industrial processes is stimulating the development of new materials for membrane manufacture. There are large expectations on the separation performance of membranes based on graphene. These membranes can exist in three different forms: a porous graphene layer, assembled graphene laminates and graphene-based composites.[1] GO is an important chemical precursor of graphene, possessing pendant functional groups such as hydroxyl, carboxyl and epoxy groups.[2] The presence of oxygen functionalities allows GO to form stable aqueous dispersions owing to electrostatic repulsion. Unlike graphene, GO can easily disperse in water and other organic solvents, forming uniform single layers, and keeping them stable even at high concentration (≈80 mg/mL) with strong mechanical properties and excellent chemical inertness.[2-3]

When preparing GO nanofiltration membranes, regularly stacked GO sheets with nano channels and amphiphilic domains are important to provide tighter molecular sieving feature resulting in high permeation flux and rejection.[4-11] The two-dimensional channels between the stacked GO nanosheets allow the water to permeate serving as molecular and ionic sieving membranes, while rejecting unwanted solutes by size exclusion process.[12-13] The recent reports of GO liquid crystals formation brought new and unique opportunities for diverse applications.[14-22] GO liquid crystals with lamellar structure might provide the desired regularly ordered sheets for filtration applications.[23] Besides their potential application in membrane manufacture, GO liquid crystals are considered excellent for the development of novel materials in optoelectronic devices, electro-optical switching, graphene-based fibers, energy storage devices, polymer nanocomposites, and oxygen reduction catalysis.[14, 16, 21, 24-29] GO, being an amphiphilic molecule self assembles under specific temperature (thermotropic) and concentration (lyotropic) and forms liquid crystals owing to long range orientational ordering. The giant anisotropy and good

dispersibility of GO promote the formation of liquid crystals in water and organic solvents such as ethanol, acetone, tetrahydrofuran, dimethylformamide (DMF) and N-methylpyrrolidone (NMP).[18, 23, 30] The material self-assembles at atomic level via π-π stacking between GO sheets and hydrogen bonding interactions.[31] Self-assembled GO nanosheets have highly enhanced physical and mechanical properties.[23] Graphene liquid crystals have also been reported using chlorosulfonic acid.[17] The self-assembly process forming liquid crystals can be easily recognized by birefringence, which results from the orientational order alongside a preferred direction, designated as director field.[32] The transition from isotropic (dark between crossed polarizer) to nematic (Schlieren texture) phase in a GO suspension on an optical polarized microscope principally depends upon GO concentration, the average aspect ratio (width/thickness) and the solvent environment, such as pH and ionic strength.[14, 20, 33-34] The formation of nematic liquid crystals is a fully "entropy driven" process.

While the majority of reports on GO liquid crystals are in water, the use of organic solvents is interesting, because it allows the incorporation of additives and crosslinkers or blending with polymers that are insoluble in water. By using ionic liquids as solvent, the advantages of organic solvents can be combined with low volatility and therefore low organic vapor emission. Moreover, particularly for membrane preparation by casting the dispersion in ionic liquids brings an important rheological advantage. The GO dispersions in water or organic solvents have low viscosity. High GO concentration is needed to reach a reasonable viscosity for casting well-ordered nanosheets leading to a defect free membrane selective layer. GO dispersions in ionic liquids are much more viscous. Diluted GO dispersions in ionic liquids can be easily cast with the expected liquid crystal order. Stable and defect free layers can be easily formed.

We report for the first time GO liquid crystals dispersed in ionic liquids. We chose ethylammonium nitrate (EAN), a protic ionic liquid, as an example, due to its similarity with water in terms of its protic nature and solvent properties such as polarity and self-assembling capability.[35] We demonstrate the formation of GO liquid crystals with viscosity adequate for casting using GO concentrations as low as 9 mg/mL. At lower GO concentration in EAN the birefringence was not observed. The rheological experiments and membrane preparation were then performed at this concentration both in EAN and water. We believe that hydrogen bondings between GO nanosheets and EAN lead to a stable, homogeneous dispersion, that can self-assemble to form nematic phase. To fully exploit the self-assembled GO sheets, membranes were cast on a polymer support by a simple doctor blade tool and were characterized for nanofiltration as illustrated in Scheme 1. Our findings should facilitate new routes for achieving GO liquid crystals from ionic liquid, help to understand the interactions leading to their formation and offer opportunities for new applications in the separation field.

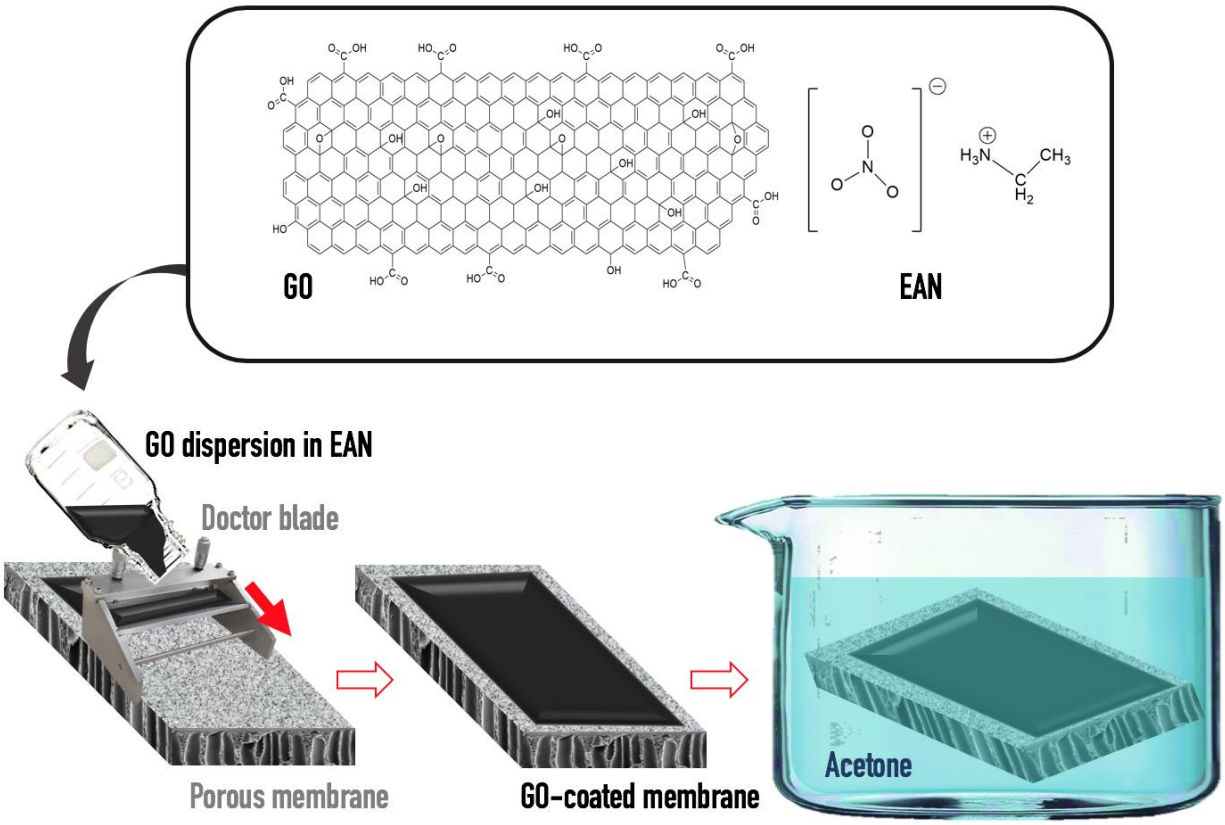

Scheme 1. GO liquid crystal dispersion in EAN, cast on a polymer support using a doctor blade and immersed in acetone to obtain nanofiltration membranes.

RESULTS AND DISCUSSION

GO was prepared from expandable graphite, as detailed in the experimental section. The aspect ratio of the resulting single layered GO sheets was preserved without the aid of ultra-sonication. This helped in producing large GO sheets and ensuring no breakage of GO sheets. The stable suspension, which exhibits anisotropic textures, facilitated the formation of liquid crystal at low concentration of GO aqueous dispersion. Figure 1a shows the SEM micrograph of large GO flakes obtained from aqueous dispersions confirms the lateral size of tens of micrometers. A minor part of the GO sheets is smaller than 10 μm. Wrinkling occurs owing to the large GO platelet size and high density of functional oxygen groups on GO plane, which facilitate the

hydrogen bond formation.[36] GO nanosheets with high aspect ratio can align parallel to each other by maximizing the packing entropy.[37] AFM was studied to assess the number of layers and quality of GO nanosheets in the aqueous dispersion. Confirming the observation by SEM, the AFM images indicate a sheet size of more than tens of micrometers in Figure 1b. The thickness profile measured is ~1.2 nm, indicating a monolayer exfoliation. The prepared GO sheets are therefore single-layered and individually dispersed in water. In this case, there is no restacking or aggregation of individual GO platelets, suggesting good exfoliation with giant lateral size of the sheets. The XRD characterization of the obtained GO and the original graphite is shown in Figure 2a. The interlayer spacing is proportional to the degree of oxidation. The XRD patterns of graphite represents a fully graphitic system with a sharp 002 peak at $2\theta = 26.4°$ and corresponding *d*-spacing of 0.34 nm, according to Bragg's law. The as prepared expandable graphite displayed similar peak with slightly expanded layer, after acid intercalation. On the other hand, the synthesized GO had a distinct peak at $2\theta = 9.1°$ with corresponding *d*-spacing of 0.97 nm. The d-spacing values are similar to those reported elsewhere for GO dry sheets, also obtained from dispersions in water.[38-40] The FTIR spectrum of GO sheets and the correspondent functional groups were identified and reported in Figure 2b. The FTIR spectrum reveals the O-H stretching vibrations (3100-3400 cm^{-1}), C=O stretching vibration (1720-1740 cm^{-1}), C=C from unoxidized C-C bonds (1610 cm^{-1}), C-O stretching vibrations (1040 cm^{-1}). This confirms that GO sheets are decorated with oxygen functional groups, following the oxidation. The UV-Vis spectrum exhibits two characteristic features, as shown in Figure 2c. The absorption peak, indicating a red shift at 231 nm, illustrates π-π^* transitions (conjugation), and a shoulder, observed around 300 nm, is attributed to the n-π^* transition of the carbonyl groups. The Raman spectroscopic measurement revealed two typical peaks seen in Figure 2d. The D and G band at

~1590 cm^{-1} and ~1340 cm^{-1} confirms the lattice distortions. XPS measurements in Figure 2e and 2f gave information on the chemical composition of GO sheets. The spectrum indicates both the C1s and O1s peaks for GO sheets with atomic concentration of 69.22 % and 29.04 %, respectively. The apparent peak at ~287 eV corresponds to graphitic carbon of GO and the peak at ~534 corresponds to oxidized carbon. This is a direct measurement of the oxygen content and the degree of oxidation obtained in the GO synthesis. The oxygen content reported here corresponds to a highly oxidized material.[38] These characterization results confirm the successful preparation of single layer exfoliated GO nanosheets in water.

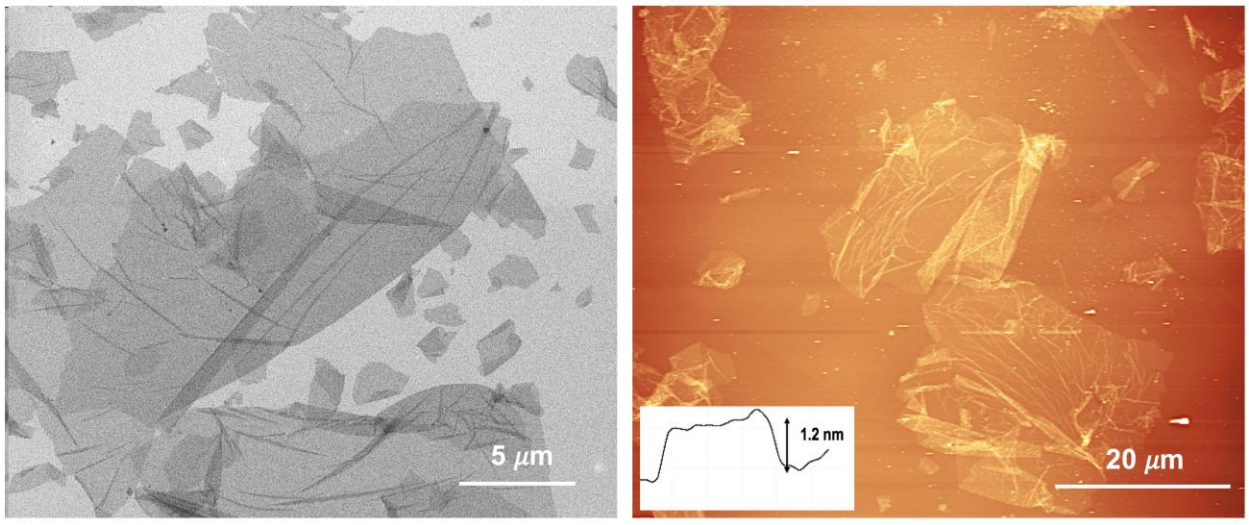

(a) (b)

Figure 1. (a) SEM and (b) AFM tapping mode images of GO sheets collected from dispersions in water (inset is the height profile of GO sheet).

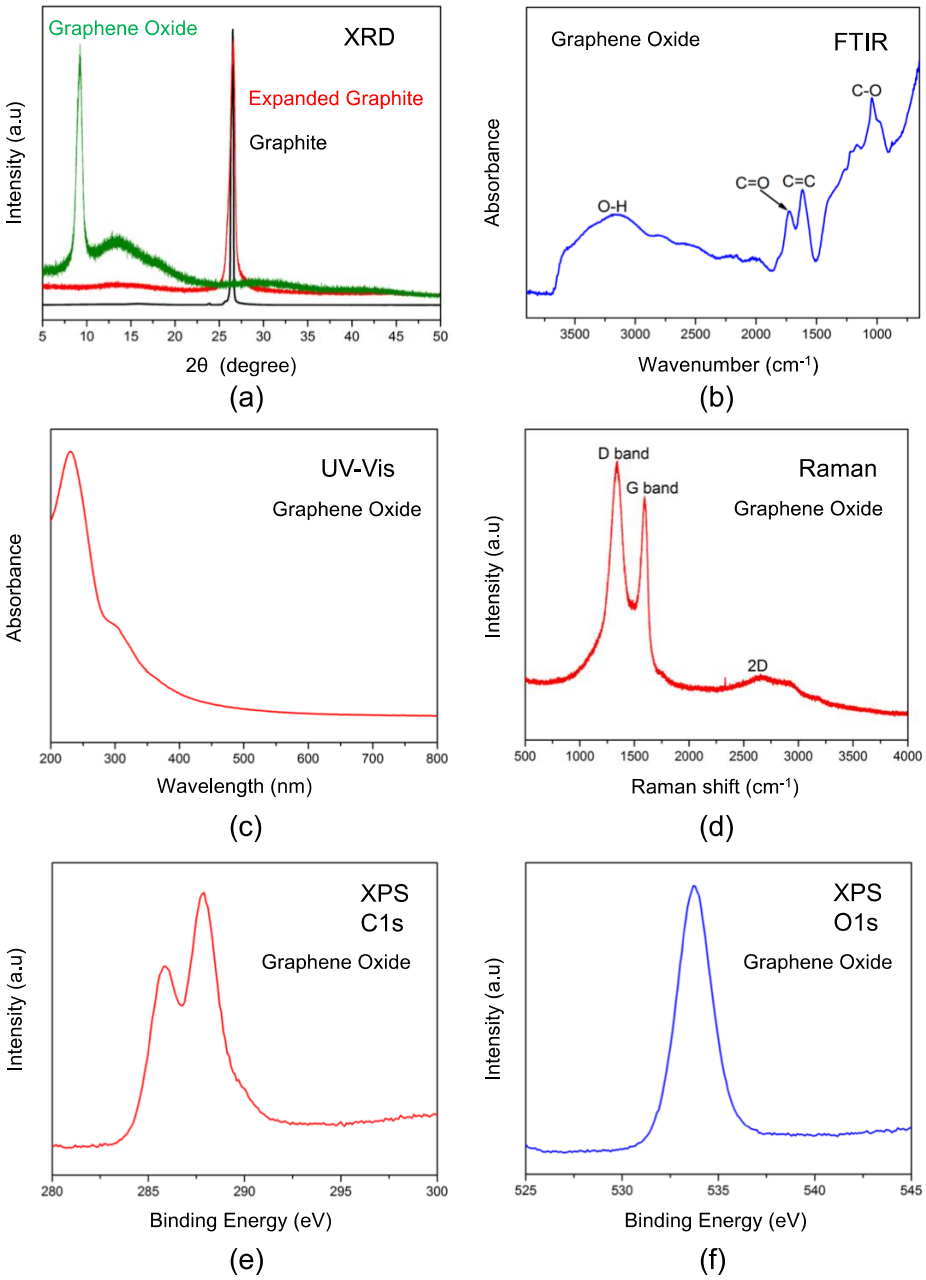

Figure 2. (a) X-ray diffraction (XRD) patterns of graphite, expandable graphite and GO; (b) FTIR spectrum of GO nanosheets; (c) UV-Vis spectrum of GO nanosheets; (d) Raman (633 nm laser excitation) spectrum of GO nanosheets; (e) and (f) XPS of GO sheets showing C 1s and O 1s peaks.

We first consider here the GO dispersibility in different media. Besides the comprehensive investigation of GO systems in water by different groups, only relatively limited studies of GO or reduced GO exfoliation and dispersion have been previously reported in another medium, such as selected organic solvents.[39, 41-42] A close matching between the surface energies of GO and solvents is important for an effective exfoliation. The surface energies of convenient solvents for exfoliation lie in the range of 40-50 mJ/m^2. The surface tension of ionic liquids such as 1-butyl-3-methylimidazolium tetrafluoroborate is 43.9 mJ/m^2 at 25 °C, which is slightly higher than that of conventional organic solvents such as N-methyl pyrrolidone (40.1 mJ/m^2).[39] Additionally, Hansen's[43] solubility and Kamlet-Taft's[44] solvent parameters have been used to rationalize the stability of reduced GO in organic solvents.[39, 42] A good dispersion of GO in organic solvents is expected to occur if the sum of the solvent $\delta_p + \delta_h$ (δ_p, Hansen's polarity cohesion parameter; δ_h, hydrogen bonding cohesion parameter) is in the range of 13~29 $MPa^{1/2}$, or if the solvent polarity parameter, $E_T(30)$,[45] is in the range of 39~53 $kcal \cdot mol^{-1}$. $E_T(30)$ indicates the solvating ability of a liquid and is related to Kamlet-Taft's parameters π^*, the polarizability of solvent, and α, the solvent's hydrogen-bond donator acidity, according to Equation 1.[45]

$$E_T(30) / kcal.mol^{-1} = 31.2 + 11.5\pi^* + 15.2\alpha \quad (1)$$

Herein, the protic ionic liquid EAN is the dispersion medium. The $E_T(30)$ and Kamlet-Taft parameters of water and EAN are similar, which suggests that EAN would be able to easily disperse GO nanosheets, as shown in Table 1. Indeed, a homogeneous GO dispersion was obtained in EAN. The exfoliated GO nanosheets after dispersion in EAN were characterized by XRD. As shown in Figure 3, the *d*-spacing of GO nanosheets after dispersion in EAN shifted to

higher values, compared to those dispersed in water. A larger interlayer distance is then promoted by the ionic liquid.

Table 1. $E_T(30)$ and Kamlet-Taft solvent parameters for water, EAN and selected organic solvents at 25 °C

Solvents	$E_T(30)$ (kcal.mol^{-1})	Kamlet-Taft parameter			Reference
		α	β	π^*	
Water	63.1	1.17	0.18	1.09	[39]
EAN	60.8	1.10	0.46	1.12	[46]
DMF	43.2	0	0.69	0.88	[39]
NMP	43.8	0	0.77	0.92	[39]

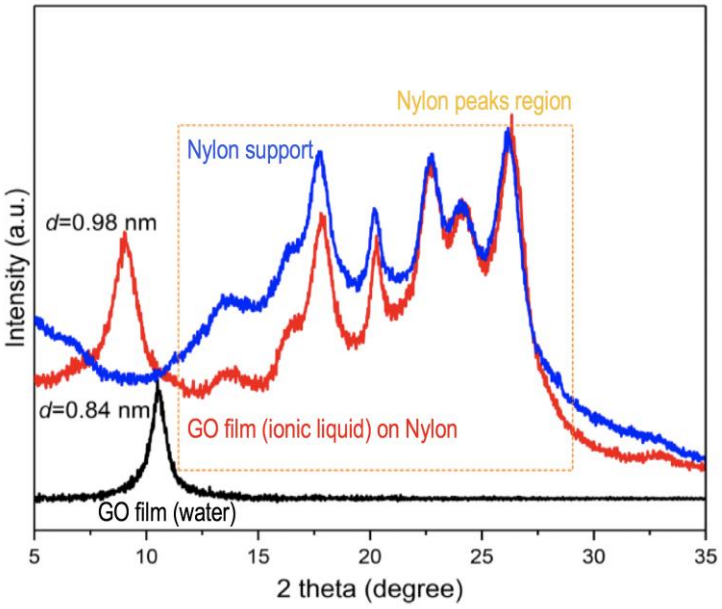

Figure 3. XRD patterns of a GO film prepared in water, an analogous film prepared in ionic liquid on a nylon porous support and the non-coated nylon support.

An effective dispersibility is essential but not the only condition for liquid crystal formation. It is important to evaluate the GO proneness to self-assemble. GO sheets have an amphiphilic character with a largely hydrophobic basal plane and hydrophilic edges.[47] GO can behave as a surfactant, having the ability to adsorb on interfaces, thus lowering the surface or interfacial tension and undergoing a self-assembly process. The amphiphilicity can be size dependent. The high degree of anisotropy and high aspect ratio of GO nanosheets render them the ability to align in a specific direction. The influence of the solvent molecules greatly impacts the structural formation of GO liquid crystal dispersion, as the solvent molecules disturb the particles interaction as a consequence of electrostatic repulsion forces.[48] Polarized Optical Microscopy is a useful characterization technique to detect anisotropy, which is indicated by birefringence.[32] Schlieren brush-like birefringence patterns have been previously seen as an indication of nematic liquid crystal phase formation in GO aqueous systems.[14, 30] A Schlieren texture was observed with various disclinations, which is a reflection of GO platelets, orienting in a preferential direction. The representative optical polarized micrographs shown in Figure 4a and 4b are an evidence of the birefringent lyotropic liquid crystals of GO in water and in EAN observed in this work. For the EAN system, the residual water content of EAN was determined by the Karl Fischer titration method. A water content lower than 0.1 wt% was detected. This is a good indication that the water is not the driving agent for the GO liquid crystal formation. A concentration of 9 mg GO/mL was chosen for our experiments in water and EAN. This is higher than the reported value (0.25 mg/mL) for isotropic-nematic transition in water[18] or dimethylformamide and lower than the concentrations previously used for GO aqueous dispersion (>40 mg/mL) for membrane preparation.[21]

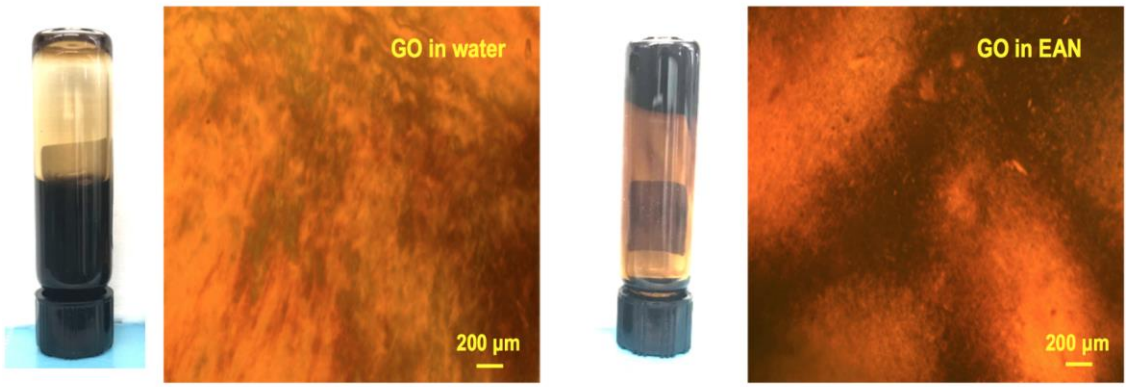

Figure 4. (a, b) Polarized optical microscopy images of GO liquid crystal dispersions in (a) water and (b) EAN; corresponding photographs of the dispersions, indicating the gel-like behavior of GO in EAN.

As previously reported for water and a few organic solvents[18], EAN is expected to interact with GO, being confined between sheets and stabilizing the assemblies the dispersion, leading to a balance of enthalpic forces and entropic contributions. Ionic liquids in general can act as an amphiphilic self-assembly media for block copolymers, leading to micelle and liquid crystalline mesophase formation, due to a "solvophobic effect".[49-50] Notably, protic ionic liquids are tunable solvents and have specific physicochemical properties by changing cations and anions. Unlike protic ionic liquids and water, aprotic ionic liquids are not capable of donating and accepting hydrogen bonded networks. EAN indeed has greater similarity with water, due to its protic nature, high polarity, high cohesive energy, which acts as a driving force for aggregation of surfactant molecules and self-assembling capability.[35, 51-53] The solvophobic force in EAN can be compared with the hydrophobic force in water, which is well dominated by the entropic contribution. The hydrophobic effect in water is a driving force for self-assembly. [18,54-56] The

process of self-assembly in general is due to the interplay of entropy and enthalpy as given in Equation 2.

$$\Delta G^{\circ}_{self\text{-}assembly} = \Delta H^{\circ}_{self\text{-}assembly} - T\Delta S^{\circ}_{self\text{-}assembly} \quad (2)$$

where $\Delta G^{\circ}_{\text{self-assembly}}$ is the free energy, $\Delta H^{\circ}_{\text{self-assembly}}$ is the enthalpy change, T is the temperature and $\Delta S^{\circ}_{\text{self-assembly}}$ is the entropy change. Besides temperature, factors contributing to self–assembly are van der Waals, hydrogen bonding and electrostatic interactions. $\Delta G^{\circ}_{\text{self-assembly}}$ has strong hydrophobic and electrostatic contributions. In the case of protic ionic liquids, the solvent itself is an ion, and so the surface charge of the assembling block copolymers or graphene oxide sheets is fully screened. The electrostatic contribution to the self-assembly due to charge in these cases becomes negligible. Hydrogen bonding and dispersive hydrophobic forces are therefore the dominant agents in the self-assembly.[49] The tendency to self-assemble can be expressed in terms of Gordon parameter, G, which is a measure of solvent cohesiveness as given in Equation 3:[57]

$$G = \gamma / V_m^{-1/3} \quad (3)$$

where γ is the air-liquid surface tension and V_m is the molar volume. Higher Gordon values are linked to better chances of forming stable liquid crystalline phases.[58] The higher the G values, the stronger is the driving force for the self-assembling process. Currently the solvent with the lowest Gordon value that can facilitate amphiphilic self-assembly is ethylammonium butyrate (EAB), also a protic ionic liquid with G = 0.576 J m^{-3}. The Gordon value for EAN (1.060 J m^{-3}) is well beyond the threshold to determine the capability to self-assemble, which is an additional indication that EAN can self-assemble GO nanosheets to form GO liquid crystals. It is expected that in GO liquid crystals, the solvent adopts a more structural arrangement between GO sheets

to balance the steric forces and repulsive forces.[18] For that, the ability of EAN to form an extensive hydrogen-bonding network is particularly important.

Herein, we compared the rheological behavior of GO in water and EAN, by studying their unique viscoelastic behavior, assessing the influence of the shear stress on the solution viscosity. A detailed investigation of rheology as a function of shear rates and volume fractions for GO liquid crystals in water has been previously reported.[37, 59] Dispersions in EAN are much more viscous, having a gel-like character even at a relatively low concentration, such as 9 mg/mL, a condition at which the equivalent dispersion in water has a predominantly liquid-like flow. The high viscosity of EAN restricts the movement of GO sheets, thus improving the stability of the liquid crystal phase.[60] A typical shear-thinning flow behavior is shown in Figure 5a, suggesting that the anisotropic GO sheets are aligned under flow. This is a common non-Newtonian behavior.[61] Gao and coworkers pioneered the rheological investigation of GO liquid crystals in water and demonstrated that in that case the shear viscosity decreases due to an isotropic-nematic transition, which they attributed to the platelets alignment in the flow direction. Similar shear-thinning behavior was reported for GO aqueous dispersion by different groups.[20-21, 62] An analogous rheological behavior was observed in our system. The viscosity is influenced by the GO composition and also by the molecular arrangements in the dispersion. The shear effect on GO liquid crystals in water and EAN is further demonstrated in Figure 5b. As the shear rate increases, a horizontal stress plateau is observed for GO in water and EAN until it reaches a constant value. It is believed that a GO network breaks down into progressively smaller flocs at high oscillating frequency to help maintaining a relatively constant stress. Further increase in shear rate increases the stress, which is due to breaking up of the flocs fully into dispersed GO flakes.[63] Similar trends were observed and reported for dispersions in water.[37, 48]

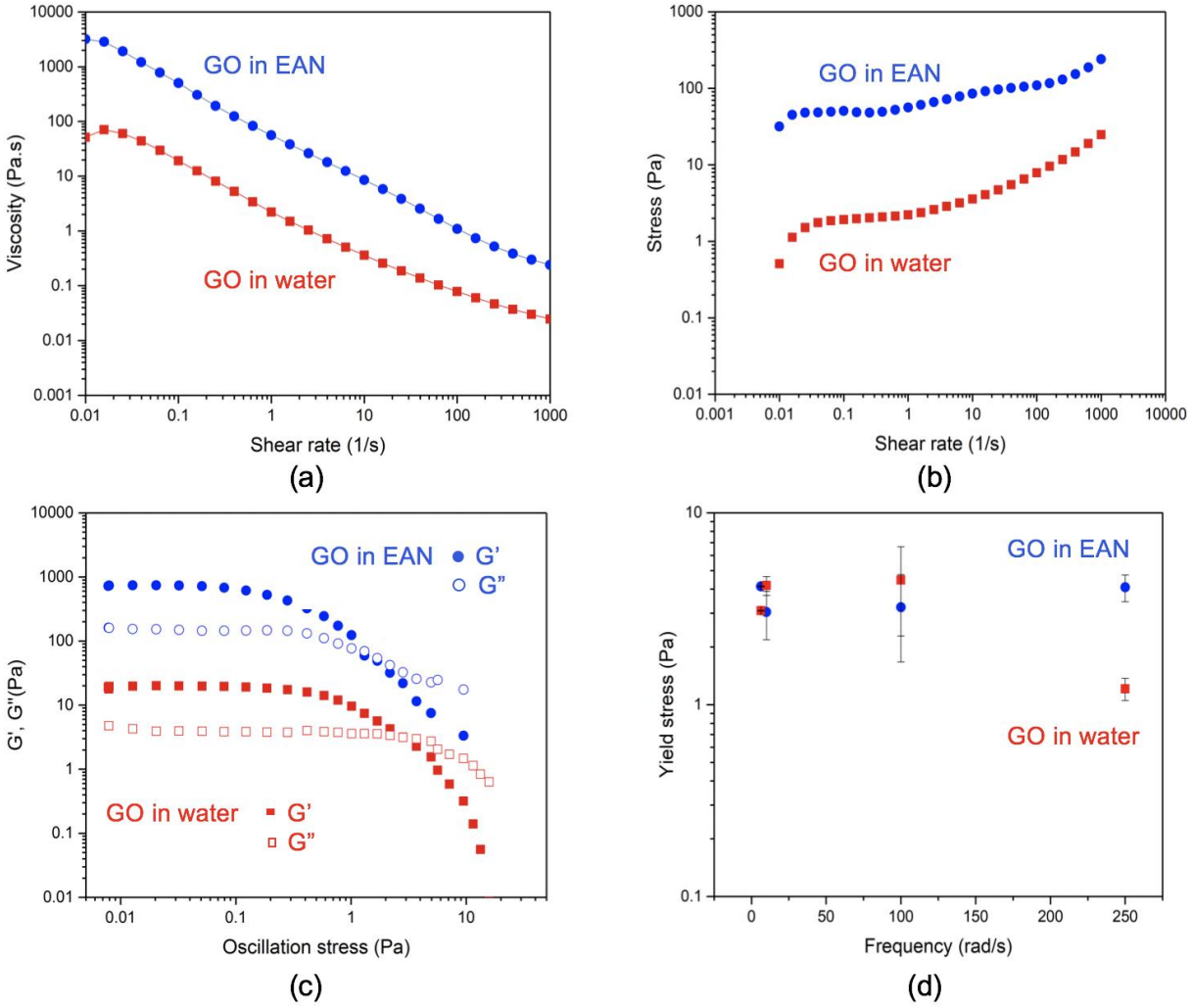

Figure 5. (a) Viscosity of GO dispersion in water and EAN as a function of shear rate. (b) Shear rate vs Shear Stress curve of GO in water and EAN (c) Storage and loss moduli measurements as a function of oscillation stress of GO dispersions in water and EAN at 10 rad/s. (d) Yield stress as a function of frequency for GO dispersions in water and EAN at 0.1% strain amplitude.

Oscillatory stress sweep measurements are performed to investigate the linear viscoelastic regime. The linear viscoelastic regime is defined as the region in which both storage modulus (G') and loss modulus (G'') are nearly constant and independent of the applied stress. The

typical oscillatory stress sweep measurements for liquid crystalline GO dispersion in water and EAN are shown in Figure 5c. Here, the G' and G'' moduli are nearly constant up to a critical stress value and, as the stress increases further, the moduli begins to decrease. Kim and coworkers[37, 64] attributed the crossover of G' and G'' to the rupture of the physical GO network. The cross over point is the condition at which the dispersion suffers a transition from a solid-like to liquid like behavior. Above this critical cross over stress, G' and G'' become strongly stress-dependent. At high concentration, the crossover point is the transition from a highly interconnected gel to a system with highly oriented and aligned GO flakes. The elastic G' (storage) and viscous G'' (loss) moduli of GO dispersion in water and EAN were investigated as a function of frequency at constant strain amplitudes of 0.1 and 1% (see Figure S1 in Supporting Information). As shown in Figure S1, only a minor increase of G' with increasing angular frequency is observed at the low-frequency range, below 100 rad/s. G' is higher than G'' in this range, characterizing a gel-like system. The gelation is a result of hydrogen bonding, π-stacking, electrostatic interaction and coordination.[65] At higher frequencies, both moduli increase, becoming more frequency-dependent. The increase of G" is more accentuated, suggesting the rupture of GO structure and therefore assuming a liquid-like behavior. Compared to a GO dispersion in water with analogous GO content, the GO dispersion in EAN exhibits higher G' being even higher than 1000 Pa. The elasticity is high. A nematic order, similar to that observed in water is probably occurring in EAN. Molecular dynamics simulation of an ionic liquid confined between graphite walls predict a solid-liquid monolayer, or a local network structure close to the graphite surface, with a hydrogen bond structure distribution different from the bulk.[66] This immobilization might also contribute to the gel-like rheological behavior we observed. As we see in our system, GO liquid crystals starts to gel or vitrify at a critical

concentration, which is lower than that observed for an aqueous GO dispersion.[60] The reason for that is that changing the ionic strength can effectively screen the repulsive electrostatic interactions and promote the gel formation.[61] A rich phase diagram with fluid, glass and gel states have been previously reported for GO dispersions in water, highly dependent on the GO concentration and of the ionic strength of the medium. A nematic phase is connected to the gel condition. The gel and glass states are promoted by competing coulombic (at the rim of the GO sheets) and dispersive interactions (in the interior). At high salt concentrations the repulsive electrostatic interactions are screened and attractive forces predominate, leading to gelation even at low GO concentration. The gel-like behavior of the GO dispersion in EAN is therefore stimulated by the high ionic strength of EAN. The individual GO nanosheets in EAN form a network of hydrogen bonds, mediated by oxygen functional groups and the protic ionic liquid.

Plots of storage and loss moduli at higher frequencies than reported in Figure 5c are shown (see Figure S2 in Supporting Information). The oscillation stress corresponding to the G'/G" cross over is practically constant (1 to 2 Pa) for GO in EAN until a frequency of 250 rad/s. At 500 and 1000 rad/s the G' and G" curves touch each other, but no crossover is observed. The cross over for GO dispersions in water is much more dependent on the angular frequency. The stress values decrease from 3 to 2 and 0.8 Pa, as the angular frequency increases from 10 to 100 and 250 rad/s. Above 250 rad/s it was not possible to measure for dispersions in water. The system was destabilized. When experiments were conducted with the same dispersion back to a low frequency condition (see Figure S3 in Supporting Information) the moduli values practically repeated the first measurements, confirming that the destabilization is not irreversible and caused by degradation. The plot of yield stress as a function of angular frequency is shown in Figure 5d, reflecting a similar observation: non-dependence of frequency for GO in EAN and a strong

dependence for GO in water. This indicates that the EAN promotes the formation of a physical network driven by the right balance of electrostatic and dispersive forces, stabilizing the GO dispersions even at relatively low GO concentration.

The viscosity, elastic and viscous moduli remain practically constant as the temperature increases (see Figure S4 in Supporting Information), at least in the investigated range of 25 to 60ºC. Above this temperature the moduli in water have a slight increase, while in EAN continue to be constant. This is probably a result of the differential changes in the balance of electrostatic and dispersive forces in the system.

High permeate flux and high selectivity with high stability are important prerequisites for a good membrane. Our ultimate goal was to exploit the GO liquid crystal phase behavior for membrane preparation, by casting the GO dispersion on a polymeric porous support. Graphene layers can be extremely thin and have the advantage of displaying nearly frictionless surface. This enables them to minimize the transport resistance and maximize the permeate flux. Our membranes were cast using a doctor blade and immersed in acetone. GO membranes prepared by casting aqueous GO liquid crystals dispersions in water have been successfully demonstrated before.[21] In the case of our dispersions in ionic liquid, a step of immersion in acetone bath is particularly important to eliminate the remaining non-volatile ionic liquid, by diffusion. By using a doctor blade to cast, the GO nanosheets are shear-aligned, forming a nematic liquid crystal phase, constituting a dense, continuous, uniform layer on the porous nylon support. The SEM images of the pure nylon support and that of the GO membrane surface are shown in Figure 6a and 6b. The thin GO layer (~ 1 μm) is clearly seen in Figure 6c. The performance of the membranes was evaluated by measuring the water permeance and the rejection of small (466-974 g/mol) molecules. XRD measurements (Figure 3) for GO liquid crystal membranes revealed

a sharp peak in a region not overlapped by those of the nylon support. The peaks around $2\theta=12^{o}$ corresponds to *d*-spacing of 0.84 and 0.98 nm, respectively for membranes obtained with GO dispersions in water and EAN. This suggests that some residual protic ionic liquid may remain between GO sheets and increase the *d*-spacing. This seems to contribute to a higher water permeance. To improve the stability, the GO layer was partially reduced by thermally heating at 100 °C under vacuum for over 24 hours as shown in Figure 6d. The membranes exhibited water permeance of 37±2 L m^{-2} h^{-1} bar^{-1} (average of 3 measurements). The rejection of Rose Bengal, Congo Red, Brilliant Blue, Indigo Carmine was evaluated. 99.9 % rejection of dyes with molecular weight larger than 697 g/mol were obtained (see Table S1 in Supplementary Information). The water permeances of the GO membranes were compared to values reported in the literature prepared from GO dispersions in water (see Table S2 in Supporting Information). The separation in the GO membranes is attributed to the direct retention of dye molecules, by physical sieving in the interlayer GO nano channels and electrostatic interaction between the negatively charged GO nanosheets.[67] Large organic molecules can be sieved by size exclusion, Donan exclusion and adsorption.

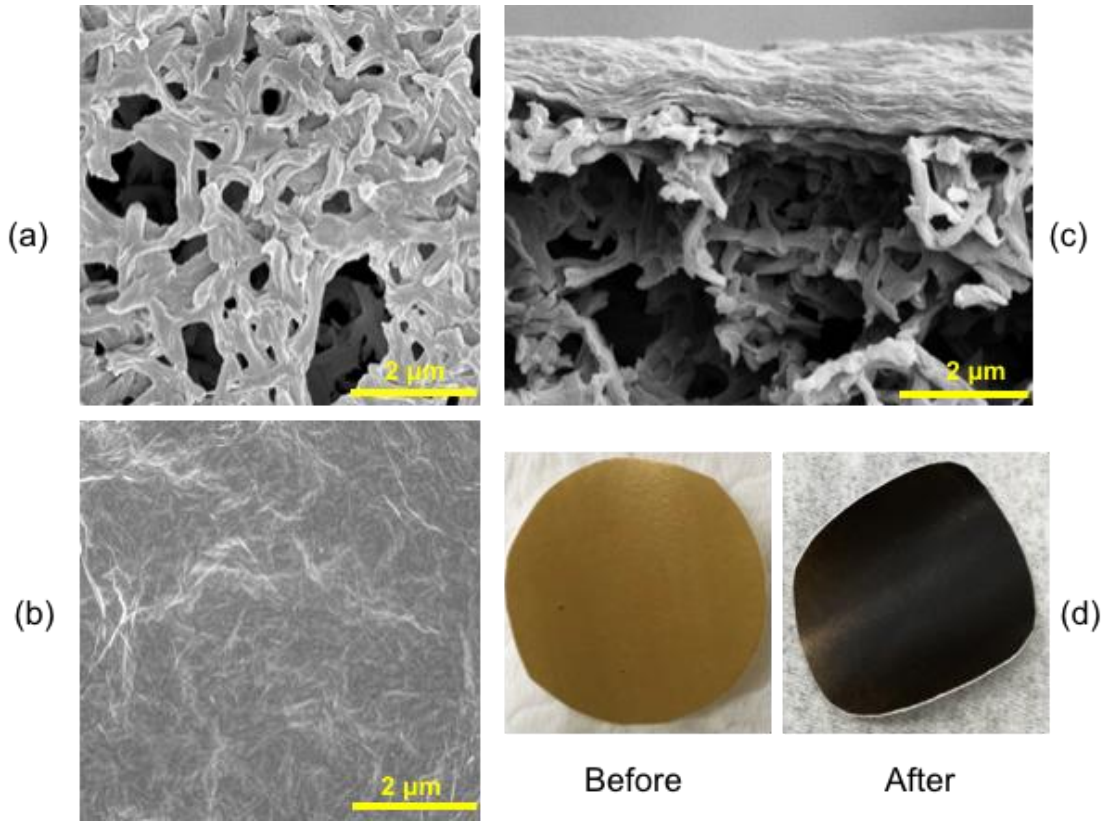

Figure 6. (a, b) SEM surface image of an (a) uncoated and (b) GO-coated nylon porous membrane; (c) cross sectional SEM image of a GO layer on a nylon porous membrane; (d) photographs of GO membranes before and after thermal reduction.

CONCLUSION

We report for the first time a stable dispersion of lyotropic GO liquid crystals in ionic liquids, employing EAN as a solvent. EAN particularly promotes a hydrogen-bonded network. The large anisotropy of the GO nanosheets lead to the formation of a colloidal liquid crystal phase in EAN, confirmed by polarized microscopy. By avoiding an ultra-sonication step, large sheets of GO with liquid crystalline nematic order were obtained with a concentration of 9 mg/mL. The

amphiphilic character of the GO sheets also contributes for the self-alignment process. The GO dispersion exhibited a non-Newtonian shear thinning behavior, typical of liquid crystal phases. A gel-like behavior was observed in rheological measurements, reflected in the elastic modulus variation with the applied stress. We produced membranes with a thin, ordered, continuous, GO selective layer by a simple casting technique. Regular structural order and stacking periodicity due to liquid crystallinity facilitated the formation of the GO membranes and led to high water permeance. We believe that our findings will enlighten the exploitation of ionic liquids as alternative solvents to form GO liquid crystals for application in separation processes as well as in other fields.

MATERIALS AND METHODS

All the chemicals were commercially available and were used as received, unless otherwise specified. Graphite flakes, sulfuric acid and 3-aminopropyltriethoxysilane were purchased from Sigma-Aldrich; nitric acid and hydrogen peroxide (H_2O_2) were supplied by VWR Chemicals; potassium permanganate ($KMnO_4$) was from Fisher Scientific. Ethylammonium nitrate (EAN) was purchased from Iolitec GmbH. Porous nylon membranes (0.2 μm pore size, 45 mm diameter) was supplied by GVS Filtration Inc.

Synthesis of GO. The synthesis of GO followed a literature method.[23] Dry graphite flakes and concentrated sulfuric acid were mixed in a round-bottomed flask and kept under stirring at 200 rpm for a few hours and concentrated nitric acid was then added into the mixture. The mixture was stirred for 1 day under constant stirring. The mixture was washed thoroughly with deionized water three times, centrifuged and dried at 60 °C to obtain graphite intercalated compounds. They were then thermally expanded at 1050 °C for 15 seconds to obtain expanded graphite. In a

typical experiment, 1 g of expanded graphite was mixed with 200 mL of sulfuric acid and stirred in a three-necked flask. 10 g of $KMnO_4$ was slowly added to the mixture and further transferred to an ice bath and stirred over a day to completely oxidize the expanded graphite. 200 mL of deionized water and 50 mL of H_2O_2 were slowly poured to the mixture. A color change to yellowish brown was observed. The obtained mixture was washed and centrifuged with HCl solution (9:1 water: HCl by volume), again washed with deionized water till the pH of the mixture becomes greater than 5. The resultant GO suspension was then exfoliated and diluted accordingly by gentle shaking without the aid of sonication.

Preparation of GO/ionic liquid suspension. The GO aqueous suspension obtained from the previous steps was used to form a GO/ionic liquid suspension via solution mixing process. The desired volumes of GO were added to deionized water and EAN in a 1:1:1 ratio and mixed well using vortex mixer. The mixture containing GO/EAN/H_2O was then transferred to a round bottomed flask and distilled using a rotary evaporator under 230 mbar vacuum at 60 °C for 8 hours to remove water. The water content of EAN used here was lower than 0.1 wt%, as determined by the Karl-Fischer titration method. The GO/EAN dispersion reported here formed liquid crystals.

GO membrane fabrication. The GO/EAN suspension was cast on a porous nylon support membrane (0.2 μm pore diameter) using doctor blade with a gap of 150 μm, immersed in an acetone bath and further dried to prepare GO membranes. The GO layers were then reduced by thermally heating at 100 °C under vacuum for 24 hours.

Characterization of GO sheets. Atomic Force Microscopy (AFM) and Scanning Electron Microscopy (SEM) analysis were performed by depositing the GO dispersion on a pre-cleaned and silanized silicon wafer. For that, 3-aminopropyltriethoxysilane was mixed with deionized

water (1:9 v/v) and 1 drop of concentrated HCl was added to the mixture. The silicon substrates were then immersed in the as prepared aqueous silane solution for 30 minutes and later thoroughly washed with deionized water. Now, the silanized silicon wafer was immersed into aqueous GO dispersion (50 μg mL^{-1}) for 5 seconds and then into deionized water in a second container for 30 seconds. The resultant substrate was air-dried over night for AFM (Bruker Dimension Icon SPM microscope) and SEM (FEI Nova Nano microscope) characterization. The AFM was carried out in tapping mode under ambient conditions. X-Ray Diffraction (XRD) studies were carried out using a powder XRD system (Bruker D8 advance) with CuKα (λ = 0.154 nm), operating at 40 keV with current of 20 mA.

The chemical analysis was performed using Attenuated Total Reflectance (ATR) Fourier Transform Infra-Red Spectroscopy (FTIR) (FTIR-iS10) in the wavenumber range of 500-4000 cm^{-1} at an average of 32 scans with 4 cm^{-1} resolution. The absorption spectra of GO were analyzed using UV-Vis Spectroscopy (UV-VIS) on a Cary 100 equipment. The Raman (Horiba-Aramis) spectrum was investigated using 633 nm HeNe laser. X-ray Photoelectron Spectroscopy (XPS) on an Amicus equipment was chosen to measure the surface elemental composition of the synthesized GO.

Characterization of EAN. The chemical structure of EAN was confirmed using Nuclear Magnetic Resonance Spectroscopy (NMR) on a 400 MHz liquid ICON NMR instrument (Figure S5). The water content of EAN was measured using the Karl-Fischer titration method.

Characterization of GO/ionic liquid. The birefringence study of the GO/ionic liquid dispersion was examined by polarized optical microscopy (Olympus BX61 Materials Microscope). Briefly, 9 mg/mL of aqueous GO dispersion was used to examine the birefringence. The dispersion was left stationary in a vial for one week. Similar procedure was

conducted for the GO/ionic liquid dispersion. Drops of the GO dispersion was transferred on a glass slide for the measurement to obtain the image. Rheological properties of aqueous GO and GO/ionic liquid were investigated using a rheometer (AR1500ex Rheometer TA instruments) with a conical shaped spindle (angle 2°, diameter 40 mm). The shear viscosity was measured at shear rates from 0.01 to 1000 s^{-1} and storage and loss modulus were measured at 0.01 to 10 Pa.

Characterization of GO liquid crystal membranes. The uniformity and continuity of the cast GO membranes were analyzed by SEM. The water permeance and rejection tests were performed using a filtration cell operated at 1 bar pressure.

ASSOCIATED CONTENT

Supporting Information Available

The Supporting Information is available free of charge on the ACS Publications website.

Additional experimental data: frequency sweep measurements at different stain amplitudes, shear viscosity and frequency sweep measurements at different temperatures, oscillatory stress sweep measurements at different frequencies and after a cycle of temperature ramp measurements, performance evaluation table, water permeance of GO membranes.

AUTHOR INFORMATION

Corresponding Author

*E-mail: suzana.nunes@kaust.edu.sa

Notes

The authors declare no competing financial interest.

ACKNOWLEDGMENTS

The authors thank King Abdullah University of Science and Technology for the financial support, in particular the Water Desalination and Reuse Center for the grants URF/1/1971-32-01 and URF/1/1971-33-01.

REFERENCES

(1) Liu, G.; Jin, W.; Xu, N., Graphene-Based Membranes. *Chem. Soc. Rev.* **2015,** *44*, 5016-5030.
(2) Leaper, S.; Abdel-Karim, A.; Faki, B.; Luque-Alled, J. M.; Alberto, M.; Vijayaraghavan, A.; Holmes, S. M.; Szekely, G.; Badawy, M. I.; Shokri, N., Flux-Enhanced Pvdf Mixed Matrix Membranes Incorporating Apts-Functionalized Graphene Oxide for Membrane Distillation. *J. Membr. Sci.* **2018,** *554*, 309-323.
(3) Dreyer, D. R.; Park, S.; Bielawski, C. W.; Ruoff, R. S., The Chemistry of Graphene Oxide. *Chem. Soc. Rev.* **2010,** *39*, 228-240.
(4) Zhu, Y.; Murali, S.; Cai, W.; Li, X.; Suk, J. W.; Potts, J. R.; Ruoff, R. S., Graphene and Graphene Oxide: Synthesis, Properties, and Applications. *Adv. Mater.* **2010,** *22*, 3906-3924.
(5) Joshi, R. K.; Carbone, P.; Wang, F. C.; Kravets, V. G.; Su, Y.; Grigorieva, I. V.; Wu, H. A.; Geim, A. K.; Nair, R. R., Precise and Ultrafast Molecular Sieving through Graphene Oxide Membranes. *Science* **2014,** *343*, 752-754.
(6) Dikin, D. A.; Stankovich, S.; Zimney, E. J.; Piner, R. D.; Dommett, G. H. B.; Evmenenko, G.; Nguyen, S. T.; Ruoff, R. S., Preparation and Characterization of Graphene Oxide Paper. *Nature* **2007,** *448*, 457-460.
(7) Hu, M.; Mi, B., Enabling Graphene Oxide Nanosheets as Water Separation Membranes. *Environ. Sci. Technol.* **2013,** *47*, 3715-3723.
(8) Hegab, H. M.; Zou, L., Graphene Oxide-Assisted Membranes: Fabrication and Potential Applications in Desalination and Water Purification. *J. Membr. Sci.* **2015,** *484*, 95-106.
(9) Hegab, H. M.; ElMekawy, A.; Barclay, T. G.; Michelmore, A.; Zou, L.; Losic, D.; Saint, C. P.; Ginic-Markovic, M., A Novel Fabrication Approach for Multifunctional Graphene-Based Thin Film Nano-Composite Membranes with Enhanced Desalination and Antibacterial Characteristics. *Sci. Rep.* **2017,** *7*, 7490.
(10) Meng, N.; Zhao, W.; Shamsaei, E.; Wang, G.; Zeng, X. K.; Lin, X. C.; Xu, T. W.; Wang, H. T.; Zhang, X. W., A Low-Pressure Go Nanofiltration Membrane Crosslinked Via Ethylenediamine. *J. Membr. Sci.* **2018,** *548*, 363-371.
(11) Mi, B., Graphene Oxide Membranes for Ionic and Molecular Sieving. *Science* **2014,** *343*, 740-742.

(12) Nair, R. R.; Wu, H. A.; Jayaram, P. N.; Grigorieva, I. V.; Geim, A. K., Unimpeded Permeation of Water through Helium-Leak-Tight Graphene-Based Membranes. *Science* **2012,** *335*, 442-444.
(13) Huang, L.; Li, Y.; Zhou, Q.; Yuan, W.; Shi, G., Graphene Oxide Membranes with Tunable Semipermeability in Organic Solvents. *Adv. Mater.* **2015,** *27*, 3797-3802.
(14) Kim, J. E.; Han, T. H.; Lee, S. H.; Kim, J. Y.; Ahn, C. W.; Yun, J. M.; Kim, S. O., Graphene Oxide Liquid Crystals. *Angew. Chem. Int. Ed.* **2011,** *50*, 3043-3047.
(15) Xu, Z.; Gao, C., Aqueous Liquid Crystals of Graphene Oxide. *ACS Nano* **2011,** *5*, 2908-2915.
(16) Xu, Z.; Gao, C., Graphene Chiral Liquid Crystals and Macroscopic Assembled Fibres. *Nat. Commun.* **2011,** *2*, 571.
(17) Behabtu, N.; Lomeda, J. R.; Green, M. J.; Higginbotham, A. L.; Sinitskii, A.; Kosynkin, D. V.; Tsentalovich, D.; Parra-Vasquez, A. N. G.; Schmidt, J.; Kesselman, E.; Cohen, Y.; Talmon, Y.; Tour, J. M.; Pasquali, M., Spontaneous High-Concentration Dispersions and Liquid Crystals of Graphene. *Nat. Nano.* **2010,** *5*, 406-411.
(18) Jalili, R.; Aboutalebi, S. H.; Esrafilzadeh, D.; Konstantinov, K.; Moulton, S. E.; Razal, J. M.; Wallace, G. G., Organic Solvent-Based Graphene Oxide Liquid Crystals: A Facile Route toward the Next Generation of Self-Assembled Layer-by-Layer Multifunctional 3d Architectures. *ACS Nano* **2013,** *7*, 3981-3990.
(19) Narayan, R.; Kim, J. E.; Kim, J. Y.; Lee, K. E.; Kim, S. O., Graphene Oxide Liquid Crystals: Discovery, Evolution and Applications. *Adv. Mater.* **2016,** *28*, 3045-3068.
(20) Yao, B.; Chen, J.; Huang, L.; Zhou, Q.; Shi, G., Base-Induced Liquid Crystals of Graphene Oxide for Preparing Elastic Graphene Foams with Long-Range Ordered Microstructures. *Adv. Mater.* **2016,** *28*, 1623-1629.
(21) Akbari, A.; Sheath, P.; Martin, S. T.; Shinde, D. B.; Shaibani, M.; Banerjee, P. C.; Tkacz, R.; Bhattacharyya, D.; Majumder, M., Large-Area Graphene-Based Nanofiltration Membranes by Shear Alignment of Discotic Nematic Liquid Crystals of Graphene Oxide. *Nat. Commun.* **2016,** *7*.
(22) Lee, K. E.; Kim, S. O., Graphene Oxide Liquid Crystals Special Issue, Editorial. *Particle and Particle Systems Characterization* **2017,** *34*.
(23) Aboutalebi, S. H.; Gudarzi, M. M.; Zheng, Q. B.; Kim, J. K., Spontaneous Formation of Liquid Crystals in Ultralarge Graphene Oxide Dispersions. *Adv. Funct. Mater.* **2011,** *21*, 2978-2988.
(24) Shen, T.-Z.; Hong, S.-H.; Song, J.-K., Electro-Optical Switching of Graphene Oxide Liquid Crystals with an Extremely Large Kerr Coefficient. *Nat. Mater.* **2014,** *13*, 394-399.
(25) Chidembo, A. T.; Aboutalebi, S. H.; Konstantinov, K.; Wexler, D.; Liu, H. K.; Dou, S. X., Liquid Crystalline Dispersions of Graphene ‐ Oxide ‐ Based Hybrids: A Practical Approach Towards the Next Generation of 3d Isotropic Architectures for Energy Storage Applications. *Part. Part. Syst. Char.* **2014,** *31*, 465-473.
(26) Liu, Z.; Xu, Z.; Hu, X.; Gao, C., Lyotropic Liquid Crystal of Polyacrylonitrile-Grafted Graphene Oxide and Its Assembled Continuous Strong Nacre-Mimetic Fibers. *Macromolecules* **2013,** *46*, 6931-6941.
(27) Lee, K. E.; Oh, J. J.; Yun, T.; Kim, S. O., Liquid Crystallinity Driven Highly Aligned Large Graphene Oxide Composites. *J. Solid State Chem.* **2015,** *224*, 115-119.

(28) Islam, M.; Chidembo, A. T.; Aboutalebi, S. H.; Cardillo, D.; Liu, H. K.; Konstantinov, K.; Dou, S. X., Liquid Crystalline Graphene Oxide/Pedot: Pss Self-Assembled 3d Architecture for Binder-Free Supercapacitor Electrodes. *Front. Energy Res.* **2014,** *2*, 31.
(29) Lee, K. E.; Kim, J. E.; Maiti, U. N.; Lim, J.; Hwang, J. O.; Shim, J.; Oh, J. J.; Yun, T.; Kim, S. O., Liquid Crystal Size Selection of Large-Size Graphene Oxide for Size-Dependent N-Doping and Oxygen Reduction Catalysis. *ACS Nano* **2014,** *8*, 9073-9080.
(30) Gudarzi, M. M.; Moghadam, M. H. M.; Sharif, F., Spontaneous Exfoliation of Graphite Oxide in Polar Aprotic Solvents as the Route to Produce Graphene Oxide - Organic Solvents Liquid Crystals. *Carbon* **2013,** *64*, 403-415.
(31) Naficy, S.; Jalili, R.; Aboutalebi, S. H.; Gorkin, R. A.; Konstantinov, K.; Innis, P. C.; Spinks, G. M.; Poulin, P.; Wallace, G. G., Graphene Oxide Dispersions: Tuning Rheology to Enable Fabrication. *Mater. Horiz.* **2014,** *1*, 326-331.
(32) Tkacz, R.; Abedin, M. J.; Sheath, P.; Mehta, S. B.; Verma, A.; Oldenbourg, R.; Majumder, M., Phase Transition and Liquid Crystalline Organization of Colloidal Graphene Oxide as a Function of Ph. *Part. Part. Syst. Char.* **2017,** *34*, 1600391-n/a.
(33) Xu, Z.; Sun, H.; Zhao, X.; Gao, C., Ultrastrong Fibers Assembled from Giant Graphene Oxide Sheets. *Adv. Mater.* **2013,** *25*, 188-193.
(34) Tkacz, R.; Oldenbourg, R.; Mehta, S. B.; Miansari, M.; Verma, A.; Majumder, M., Ph Dependent Isotropic to Nematic Phase Transitions in Graphene Oxide Dispersions Reveal Droplet Liquid Crystalline Phases. *Chem. Commun.* **2014,** *50*, 6668-6671.
(35) Greaves, T. L.; Drummond, C. J., Protic Ionic Liquids: Properties and Applications. *Chem. Rev.* **2008,** *108*, 206-237.
(36) Zheng, Q.; Geng, Y.; Wang, S.; Li, Z.; Kim, J.-K., Effects of Functional Groups on the Mechanical and Wrinkling Properties of Graphene Sheets. *Carbon* **2010,** *48*, 4315-4322.
(37) Kumar, P.; Maiti, U. N.; Lee, K. E.; Kim, S. O., Rheological Properties of Graphene Oxide Liquid Crystal. *Carbon* **2014,** *80*, 453-461.
(38) Marcano, D. C.; Kosynkin, D. V.; Berlin, J. M.; Sinitskii, A.; Sun, Z.; Slesarev, A.; Alemany, L. B.; Lu, W.; Tour, J. M., Improved Synthesis of Graphene Oxide. *ACS Nano* **2010,** *4*, 4806-4814.
(39) Zhang, B.; Ning, W.; Zhang, J.; Qiao, X.; Zhang, J.; He, J.; Liu, C. Y., Stable Dispersions of Reduced Graphene Oxide in Ionic Liquids. *J. Mater. Chem.* **2010,** *20*, 5401-5403.
(40) Cai, D.; Song, M., Preparation of Fully Exfoliated Graphite Oxide Nanoplatelets in Organic Solvents. *J. Mater. Chem.* **2007,** *17*, 3678-3680.
(41) Hernandez, Y.; Nicolosi, V.; Lotya, M.; Blighe, F. M.; Sun, Z.; De, S.; McGovern, I. T.; Holland, B.; Byrne, M.; Gun'Ko, Y. K.; Boland, J. J.; Niraj, P.; Duesberg, G.; Krishnamurthy, S.; Goodhue, R.; Hutchison, J.; Scardaci, V.; Ferrari, A. C.; Coleman, J. N., High-Yield Production of Graphene by Liquid-Phase Exfoliation of Graphite. *Nat. Nano.* **2008,** *3*, 563-568.
(42) Park, S.; An, J.; Jung, I.; Piner, R. D.; An, S. J.; Li, X.; Velamakanni, A.; Ruoff, R. S., Colloidal Suspensions of Highly Reduced Graphene Oxide in a Wide Variety of Organic Solvents. *Nano Lett.* **2009,** *9*, 1593-1597.
(43) Hansen, C. M., *Hansen Solubility Parameters: A User's Handbook*. CRC press: 2002.
(44) Kamlet, M. J.; Taft, R., The Solvatochromic Comparison Method. I. The. Beta.-Scale of Solvent Hydrogen-Bond Acceptor (Hba) Basicities. *J. Am. Chem. Soc.* **1976,** *98*, 377-383.
(45) Reichardt, C., Polarity of Ionic Liquids Determined Empirically by Means of Solvatochromic Pyridinium N-Phenolate Betaine Dyes. *Green Chem.* **2005,** *7*, 339-351.

(46) Mancini, P. M.; Fortunato, G. G.; Vottero, L. R., Molecular Solvent/Ionic Liquid Binary Mixtures: Designing Solvents Based on the Determination of Their Microscopic Properties. *Phys. Chem. Liq.* **2004,** *42*, 625-632.
(47) Kim, J.; Cote, L. J.; Kim, F.; Yuan, W.; Shull, K. R.; Huang, J., Graphene Oxide Sheets at Interfaces. *J. Am. Chem. Soc.* **2010,** *132*, 8180-8186.
(48) Jalili, R.; Aboutalebi, S. H.; Esrafilzadeh, D.; Konstantinov, K.; Razal, J. M.; Moulton, S. E.; Wallace, G. G., Formation and Processability of Liquid Crystalline Dispersions of Graphene Oxide. *Mater. Horiz.* **2014,** *1*, 87-91.
(49) Greaves, T. L.; Drummond, C. J., Ionic Liquids as Amphiphile Self-Assembly Media. *Chem. Soc. Rev.* **2008,** *37*, 1709-1726.
(50) Madhavan, P.; Sougrat, R.; Behzad, A. R.; Peinemann, K.-V.; Nunes, S. P., Ionic Liquids as Self-Assembly Guide for the Formation of Nanostructured Block Copolymer Membranes. *J. Membr. Sci.* **2015,** *492*, 568-577.
(51) Greaves, T. L.; Weerawardena, A.; Fong, C.; Drummond, C. J., Formation of Amphiphile Self-Assembly Phases in Protic Ionic Liquids. *J. Phys. Chem. B* **2007,** *111*, 4082-4088.
(52) Evans, D. F.; Yamauchi, A.; Roman, R.; Casassa, E. Z., Micelle Formation in Ethylammonium Nitrate, a Low-Melting Fused Salt. *J. Colloid Interface Sci.* **1982,** *88*, 89-96.
(53) Evans, D. F.; Yamauchi, A.; Wel, G. J.; Bloomfield, V. A., Micelle Size in Ethylammonium Nitrate as Determined by Classical and Quasi-Elastic Light Scattering. *J. Phys. Chem.* **1983,** *87*, 3537-3541.
(54) Southall, N. T.; Dill, K. A.; Haymet, A. D. J., A View of the Hydrophobic Effect. *J. Phys. Chem. B* **2002,** *106*, 521-533.
(55) Chandler, D., Interfaces and the Driving Force of Hydrophobic Assembly. *Nature* **2005,** *437*, 640.
(56) Meyer, E. E.; Rosenberg, K. J.; Israelachvili, J., Recent Progress in Understanding Hydrophobic Interactions. *Proc. Natl. Acad. Sci.* **2006,** *103*, 15739-15746.
(57) Evans, D. F., Self-Organization of Amphiphiles. *Langmuir* **1988,** *4*, 3-12.
(58) Lee, W. B.; Mezzenga, R.; Fredrickson, G. H., Anomalous Phase Sequences in Lyotropic Liquid Crystals. *Phys. Rev. Lett.* **2007,** *99*, 187801.
(59) Lin, F.; Tong, X.; Wang, Y.; Bao, J.; Wang, Z. M., Graphene Oxide Liquid Crystals: Synthesis, Phase Transition, Rheological Property, and Applications in Optoelectronics and Display. *Nanoscale Res. Lett.* **2015,** *10*, 1-16.
(60) Shim, Y. H.; Lee, K. E.; Shin, T. J.; Kim, S. O.; Kim, S. Y., Wide Concentration Liquid Crystallinity of Graphene Oxide Aqueous Suspensions with Interacting Polymers. *Mater. Horiz.* **2017,** *4*, 1157-1164.
(61) Konkena, B.; Vasudevan, S., Glass, Gel, and Liquid Crystals: Arrested States of Graphene Oxide Aqueous Dispersions. *J. Phys. Chem. C* **2014,** *118*, 21706-21713.
(62) Yang, X.; Guo, C.; Ji, L.; Li, Y.; Tu, Y., Liquid Crystalline and Shear-Induced Properties of an Aqueous Solution of Graphene Oxide Sheets. *Langmuir* **2013,** *29*, 8103-8107.
(63) Vallés, C., Rheology of Graphene Oxide Dispersions. In *Graphene Oxide: Fundamentals and Applications*, John Wiley & Sons, Ltd.: United States,, 2016; pp 121-146.
(64) Shih, W. Y.; Shih, W. H.; Aksay, I. A., Elastic and Yield Behavior of Strongly Flocculated Colloids. *J. Am. Ceram. Soc.* **1999,** *82*, 616-624.
(65) Bai, H.; Li, C.; Wang, X.; Shi, G., On the Gelation of Graphene Oxide. *J. Phys. Chem. C* **2011,** *115*, 5545-5551.

(66) Sha, M.; Wu, G.; Fang, H.; Zhu, G.; Liu, Y., Liquid-to-Solid Phase Transition of a 1,3-Dimethylimidazolium Chloride Ionic Liquid Monolayer Confined between Graphite Walls. *J. Phys. Chem. C* **2008,** *112*, 18584-18587.
(67) Zhang, Y.; Chung, T. S., Graphene Oxide Membranes for Nanofiltration. *Curr. Opin. Chem. Eng.* **2017,** *16*, 9-15.

TABLE OF CONTENTS